Brain, Behavior, and Immunity xxx (xxxx) xxx–xxx

Contents lists available at ScienceDirect

Brain, Behavior, and Immunity

journal homepage: www.elsevier.com/locate/ybrbi

Full-length Article

# Post-operative pain in mice is prolonged by diet-induced obesity and rescued by dietary intervention

Owein Guillemot-Legris[a], Baptiste Buisseret[a], Valentin Mutemberezi[a], Emmanuel Hermans[b], Ronald Deumens[b], Mireille Alhouayek[a], Giulio G. Muccioli[a,*]

[a] Bioanalysis and Pharmacology of Bioactive Lipids Research Group, Louvain Drug Research Institute, Université catholique de Louvain, Avenue Mounier 72 (B1.72.01), 1200 Brussels, Belgium
[b] Neuropharmacology Group, Institute of Neuroscience, Université catholique de Louvain, Avenue Hippocrate 54 (B1.54.10), 1200 Brussels, Belgium

ARTICLE INFO

*Keywords:*
Sciatic nerve
Chronic pain
Microglia
Astrocytes
Neuroinflammation
High fat diet

ABSTRACT

The prevalence of obesity has increased at an alarming rate during past decades. Obesity is associated with pathophysiological disorders that can evolve and increase the risk of heart disease, diabetes and hypertension. While the impact of diabetes on post-operative recovery is now known, the consequences of obesity on post-operative pain remain much less explored. Here, we show that obesity affects post-operative pain resolution and leads to a chronic pain state in mice. Several mechanisms were identified as implicated in the prolonged post-operative pain. Indeed, we found that following a hind paw incision, high fat diet prolonged glial cell activation in the spinal cord. It also altered the expression of neurotrophins and increased inflammatory and endoplasmic reticulum stress markers in both central and peripheral nervous systems. Moreover, we show that a dietary intervention, leading to weight reduction and decreased inflammation, was able to restore normal pain sensitivity in mice suffering from chronic pain for more than 10 weeks. In conclusion, our data demonstrate that obesity is responsible for pain chronicization. This is clearly of importance in a clinical post-operative setting.

## 1. Introduction

Surgical procedures involve incision(s) hence a trauma of the tissues resulting in a local inflammatory response and a painful experience that eventually resolves. However, depending on the surgical procedure, chronic post-operative pain prevalence in the general population ranges from 10 to 50% (Chapman and Vierck, 2017; Deumens et al., 2013). Indeed, sometimes, the pain does not recede and results in a chronic pain state affecting the quality of life of patients (Kehlet et al., 2006; Reddi and Curran, 2014). Post-operative pain perception derives from the injury site and is relayed and tuned by the peripheral and central nervous systems. These processes can be affected by different factors, including, among others, inflammation, neurotrophin expression and endoplasmic reticulum stress (Inceoglu et al., 2015; Pezet and McMahon, 2006; White et al., 2005).

Obesity is a major health issue of modern societies and, according to epidemiological projections, this will only worsen (Wang et al., 2011). Obesity is one symptom of a cohort of pathophysiological disorders known as the metabolic syndrome encompassing metabolic disturbances such as dyslipidemia, altered cholesterol metabolism, glucose intolerance and a low grade inflammatory state (Esser et al., 2014; Lumeng and Saltiel, 2011). Over time, this metabolic syndrome can evolve towards type 2 diabetes (Lumeng and Saltiel, 2011; O'Neill and O'Driscoll, 2015). One of the most common side effects of diabetes is impaired wound-healing and occurrence of painful neuropathies (DeFronzo et al., 2015; Peltier et al., 2014). Indeed, diabetic patients are more prone to surgical complications and post-operative pain (Rajamaki et al., 2015). However, much less is known on post-operative pain in obesity. As obese patients represent an increasingly large proportion of the population, the need to shed light on this question is essential.

To study the effects of obesity in its own right on post-operative pain, we used the hind paw incision model in mouse. The procedure consists in an incision where the skin and muscles of the hind paw are cut and the skin is sewn back (Jang et al., 2011). This animal model is characterized by a self-resolving mechanical hyperalgesia (Brennan et al., 1996; Sandkuhler, 2009). Using this model, we demonstrate that diet-induced obesity results in a drastic increase of post-operative pain duration that can be rescued by a diet intervention.

* Corresponding author at: Bioanalysis and Pharmacology of Bioactive Lipids Research Group (BPBL), Louvain Drug Research Institute (LDRI), Université catholique de Louvain (UCL), Av. E. Mounier, 72 (B1.72.01), 1200 Bruxelles, Belgium.
*E-mail address:* giulio.muccioli@uclouvain.be (G.G. Muccioli).

https://doi.org/10.1016/j.bbi.2018.07.022
Received 20 May 2018; Received in revised form 8 July 2018; Accepted 25 July 2018

**Table 1**
Key parameters of the three studies.

| | Surgery | Date of sacrifice | Diet switch |
|---|---|---|---|
| First experiment | Sham or HPI | 18 days post-surgery | / |
| Second experiment | HPI | 4 days post-HPI or 13 days post-HPI | / |
| Third experiment | HPI | 44 days post-HPI or 162 days post-HPI | No switch or HFD to standard diet on the day of HPI or HFD to standard diet 10 weeks after HPI |

## 2. Materials and methods

### 2.1. Animals and diets

Nine-week-old male C57BL/6J mice (Janvier) were housed in a controlled environment (12-h day light cycle, lights off at 6 pm, controlled temperature and humidity). Upon arrival, all mice were acclimated for 1 week. Scheme representing the timelines of these three experiments are depicted in SI Fig. 1 and important parameters are included in Table 1.

For the first study, mice were randomly split into four groups in order to obtain groups with similar weight. The first two groups were given free access to a standard diet (AIN 93-M, Research Diets, New Brunswick, USA) (soybean oil-based, 9% kcal from fat) and the remaining two groups were given free access to a high fat diet (HFD) (D12492, Research Diets, New Brunswick, USA) (lard-based, 60% kcal from fat) for the duration of the experiment (60 days + 18 days) (Everard et al., 2014; Guillemot-Legris et al., 2016a; Guillemot-Legris et al., 2016b). After 60 days on their respective diets, one group of mice fed a standard chow and one group of mice fed a HFD underwent the hind paw incision (HPI) procedure whereas the two remaining groups were sham-operated. Eighteen days after the operation (HPI or sham) all mice were euthanized.

For the second study, mice were randomly split into four groups. The first two groups were given free access to the standard diet and the remaining two groups were given free access to the HFD for the duration of the experiment (60 days + 4 days or 60 days + 13 days). After 60 days on their respective diets, all mice underwent the HPI operation. Four days after the HPI, one standard chow-fed group and one HFD-fed group were euthanized. The remaining two groups were euthanized thirteen days after the HPI operation (see SI Fig. 1).

For the third study, mice were randomly split into three groups. They were all given free access to the HFD. After 60 days, all mice underwent the HPI operation. On the day of the operation, one group was switched to standard chow (H-C d0). 10 weeks after the HPI another group was switched to standard chow (H-C). Finally, the remaining group was maintained under HFD throughout the experiment (H-H) (see SI Fig. 1).

For all studies, each group included 10 mice except for H-C and H-H groups of the third experiment where 5 mice were included. Mice were anesthetized using isoflurane after a 6 h fasting period. After euthanasia, the spinal cord, brainstem, sciatic nerve, paw skin and liver were carefully and rapidly recovered and snap-frozen in liquid nitrogen, except for a section of the spinal cord which was fixed into 4% paraformaldehyde (PFA). The different adipose tissue depots (subcutaneous adipose tissue (SAT), visceral adipose tissue (VAT), epididymal adipose tissue (EAT), and brown adipose tissue (BAT)) were harvested and weighed. All the tissues collected were stored at −80 °C until further analysis. For all three studies, all animals were used to conduct all subsequent analysis (tactile hyperalgesia throughout the study as well as metabolic parameters, RT-qPCR and histology on tissues recovered at the time of sacrifice and stored appropriately).

We performed these studies in accordance with the European recommendation 2010/63/EU (which was transformed into the Belgian Law of May 29, 2013), regarding the protection of laboratory animals. The local ethics committee approved the protocol of the study (study agreement 2010/UCL/MD/022; lab agreement LA1230314).

### 2.2. Hind paw incision procedure

Animals were anesthetized using isoflurane. The plantar side of the left hind paw was sterilized and a 0.5 cm longitudinal incision, starting 0.2 cm below the heel and extending toward the toes, was made with a number 11 blade, through skin and fascia of the plantar side of the left hind paw. The plantaris muscle was then elevated and longitudinally incised, leaving the muscle origin and insertion intact. The skin was then closed with a single suture. At the end of the surgery, anesthesia was stopped and animals were allowed to recover. The sham-operated groups followed the same steps except for the incision.

### 2.3. Tactile hyperalgesia assessment

We assessed tactile hyperalgesia using von Frey filaments as previously described (Hoeber et al., 2015). In a calm environment, mice were trained to the test prior to the beginning of each study for a 14 days period. Before each testing session, mice were placed in a translucent plastic box with a wire mesh flat bottom and given 15 min for acclimation (time necessary for a decrease in exploratory and grooming behaviors). Von Frey filaments were applied to the mid plantar hind paw with a series of filaments (0.04, 0.07, 0.16, 0.4, 0.6, 1, 2 (force in gram)) and starting with 0.4. Filaments were applied once for 5 s and tactile hyperalgesia was assessed using the up-down method described by Chaplan (Chaplan et al., 1994). Results are presented as the bending force necessary to evoke paw withdrawal 50% of the time. Both ipsi- and contra-lateral paws were assessed and one paw was completely tested before testing the other paw. The investigator was blinded regarding the type of surgery (sham or HPI).

### 2.4. Glycaemia

Mice were anesthetized using isoflurane after a 6 h fasting period and blood collected. Plasma glucose was quantified, following manufacturer's instructions, in the vena cava using the Glucose GOD FS kit (DiaSys Diagnostic and Systems, Holzheim, Germany), which is based on an enzymatic reaction coupled with a spectrophotometric detection of the end-product.

### 2.5. Liver triglycerides and cholesterol quantification

DiaSys Diagnostic and Systems kits (Holzheim, Germany) were used to quantify the total cholesterol and triglycerides content of the liver after a chloroform–methanol lipid extraction (Guillemot-Legris et al., 2016b).

### 2.6. RNA preparation and RT-qPCR analysis

Total RNA from tissues was extracted using TriPure reagent (Roche, Basel, Switzerland) according to the manufacturer's instructions. cDNA was synthesized using an RT kit (Promega, GoScript™ Reverse Transcription System) from 1 µg of total RNA. qPCR was performed

**Table 2**
Primer sequences.

| Gene | MGI id | Product | Forward primer (5′–3′) | Reverse primer (5′–3′) |
|---|---|---|---|---|
| *Arg1* | 88,070 | Arg1 | GGTTCTGGGAGGCCTATCTT | TGAAAGGAGCCCTGTCTTGT |
| *Atf4* | 88,096 | Atf4 | GGCTATGGATGATGGCTTGG | ACAGAGCATCGAAGTCAAACTC |
| *Bdnf* | 88,145 | Bdnf | GGTCACAGCGGCAGATAAA | TGGGATTACACTTGGTCTCGT |
| *Itgax* | 96,609 | Cd11c | ACGTCAGTACAAGGAGATGTTGGA | ATCCTATTGCAGAATGCTTCTTTACC |
| *Ddit3* | 109,247 | CHOP | GAGCTGGAAGCCTGGTATG | TGATTCTTCCTCTTCGTTTCCTG |
| *Adgre1* | 106,912 | F4/80 | TGACAACCAGACGGCTTGTG | CAGGCGAGGAAAAGATAG |
| *Slc2a4* | 95,758 | Glut4 | TCGCTGGTTTCTCCAACTG | GGAGGACGGCAAATAGAAGG |
| *Il1b* | 96,543 | IL-1β | TGTCTTTCCCGTGGACCTTC | CCAGCAGGTTATCATCATCATCCC |
| *Il6* | 96,559 | IL-6 | ACAAGTCGGAGGCTTAATTACACAT | TTGCCATTGCACAACTCTTTTC |
| *Ccl2* | 98,259 | MCP-1 | GTCCCAAAGAAGCTGTAGTTTTTG | ATGTATGTCTGGACCCATTCC |
| *Ngf* | 97,321 | Ngf | ATGCTGGACCCAAGCTCAC | CTGCCTGTACGCCGATCAAA |
| *Ntf3* | 97,380 | NT-3 | TCACCACGGAGGAAACGCTA | GTCACCCACAGGCTCTCACT |
| *Pck1* | 97,501 | PEPCK | ACCTCCTGGAAGAACAAGGA | CTCATGGCTGCTCCTACAAA |
| *Rpl19* | 98,020 | Rpl19 | TGACCTGGATGAGAAGGATGAG | CTGTGATACATATGGCGGTCAATC |
| *XBP1* | 98,970 | sXBP1[a] | CTGAGTCCGAATCAGGTGCAG | GTCCATGGGAAGATGTTCTGG |
| *Tnf* | 104,798 | TNFα | CTACTGAACTTCGGGGTGATC | TGAGTGTGAGGGTCTGGGC |

[a] Primers designed in order to amplify only the spliced variant of XBP1 also used in (Lu et al., 2016).

with a StepOnePlus instrument and software (Applied Biosystems, Foster City, CA, USA). PCR reactions were run using a SYBR Green mix (Promega, GoTaq® qPCR Master Mix). We measured each sample in duplicate during the same run. The following conditions were used for amplification: an initial holding stage of 10 min at 95 °C, then 45 cycles consisting of denaturation at 95 °C for 3 s, annealing at 60 °C for 26 s, and extension at 72 °C for 10 s. Products were analyzed by performing a melting curve at the end of the PCR reaction. Data are normalized to the 60S ribosomal protein L19 (RPL19) mRNA) expression (Alhouayek et al., 2013; Guillemot-Legris et al., 2016a) and analyzed using the ΔΔCt method. The M1-M2 ratio was calculated for each sample as follows: Ratio = (Ct RPL19 − Ct Arg1)/(Ct RPL19 − Ct CD11c) therefore a high number indicates a low expression of Arg1 and/or a high expression of CD11c hence a more M1-type polarization of macrophage in the tissue considered for a given sample. Sequences of the primers used are listed in Table 2.

### 2.7. Immunohistology

During the sacrifice, the L3-5 region of the spinal cord was transferred to a solution of 4% PFA in PBS and stored at 4 °C for 24 h. Cryopreservation was performed by incubation in a solution of 20% sucrose in PBS for a further 24 h at 4 °C. Finally, tissues were embedded in Tissue-Tek (Sakura Finetek, Zoeterwoude, The Netherlands) and kept at −80 °C (Guillemot-Legris et al., 2016a). Sections were cut (30 µm) using a cryostat and then used for the detection of ionized calcium binding adaptor molecule 1 (Iba-1) positive cells (microglia) and glial fibrillary acidic protein (GFAP) positive cells (astrocytes). The sections were incubated in blocking solution containing 5% normal donkey serum and 1% Triton X-100 (Sigma-Aldrich, Seelze, Germany) in PBS for 60 min. The primary antibodies, rabbit anti-Iba1 (RRID: AB_2665520 Wako Laboratory Chemicals, Japan) (1:1000 in PBS/triton 1%) and direct rat anti-GFAP (RRID: AB_2314539, Sigma) (1:250 in PBS/triton 1%), were applied for 12 h at 4 °C. Tissues were then rinsed three times with PBS. The secondary antibody anti-rabbit Alexa 488 (Thermo Fisher Scientific) (1:100) was applied for 1 h at room temperature. Tissues were washed with PBS and nuclei were stained using Hoescht. Slides were mounted using Dako Fluorescence Mounting Medium. Stained slides were digitized using a Mirax Midi scanner (Carl Zeiss Micro-Imaging). Image acquisition was executed with Mirax Scan software (Zeiss). The obtained images of laminae I and II of the dorsal spinal horn (both ipsi and contralateral) were analyzed by a researcher blinded to the treatment using ImageJ software (http://imagej.nih.gov/ij/) (Guillemot-Legris et al., 2016a).

### 2.8. Sciatic nerve explants

Five 3-month old C57Bl6/J mice were euthanized by isoflurane and cervical dislocation. The sciatic nerve was rapidly exposed from spinal cord to the knee and ligated at both extremities using sutures (Dermalon, 4-0, Covidien™). The sciatic nerve was then harvested by cutting between the suture and proximal insertion and between suture and sciatic trifurcation. For each mouse, both sciatic nerves were recovered. Excess fat and connective tissue were removed. The sciatic nerve ligated at the two extremities was incubated in DMEM-F12 media (containing 15% FBS and 100 units/mL of penicillin and 100 µg/mL of streptomycin) for 1 h. Sciatic nerve explants were then incubated with fresh culture medium in the absence or presence of lipopolysaccharides (LPS) (10 ng/mL, from E. coli 055:B5) in order to mimic the peripheral inflammatory state found during high-fat diet-induced endotoxemia. After 6 h of incubation, the media was removed and the explants were transferred to TriPure (Roche) for mRNA analysis (see above).

### 2.9. Statistical analysis

All data are presented as mean ± SEM. Statistical analysis was performed using GraphPad Prism version 7.0 for Windows (San Diego, CA). Sample size was determined based on a power analysis. For the first and second study, we used a two-way ANOVA followed by Tukey's post-hoc test for comparison of RT-qPCR results, immunohistology, adipose depots weights as well as glucose, TG and cholesterol quantification. For the first study, von Frey and weight follow up results were compared using a two-way ANOVA for repeated measures followed by Tukey's post-hoc test. For the second study, von Frey and weight follow up results were compared using a two-way ANOVA for repeated measures followed by Sidak's post-hoc test. For the third study, RT-qPCR results, adipose depots weight and liver TG and cholesterol levels were compared using a two-tailed Mann-Whitney test. von Frey and weight follow-up were analyzed using a two-way ANOVA for repeated measures followed by Tukey's post-hoc test. Finally, correlations between inflammatory markers and neurotrophins in the sciatic nerve, in both studies I and II, were performed using the Spearman correlation test. For all statistical tests, statistical significance was taken when $P < 0.05$ and a trend was suggested when $P < 0.1$.

## 3. Results

### 3.1. Obesity affects post-operative pain

To obtain lean and obese phenotypes, we fed mice either a standard chow or a high fat diet (HFD). After 60 days, HFD-fed mice developed

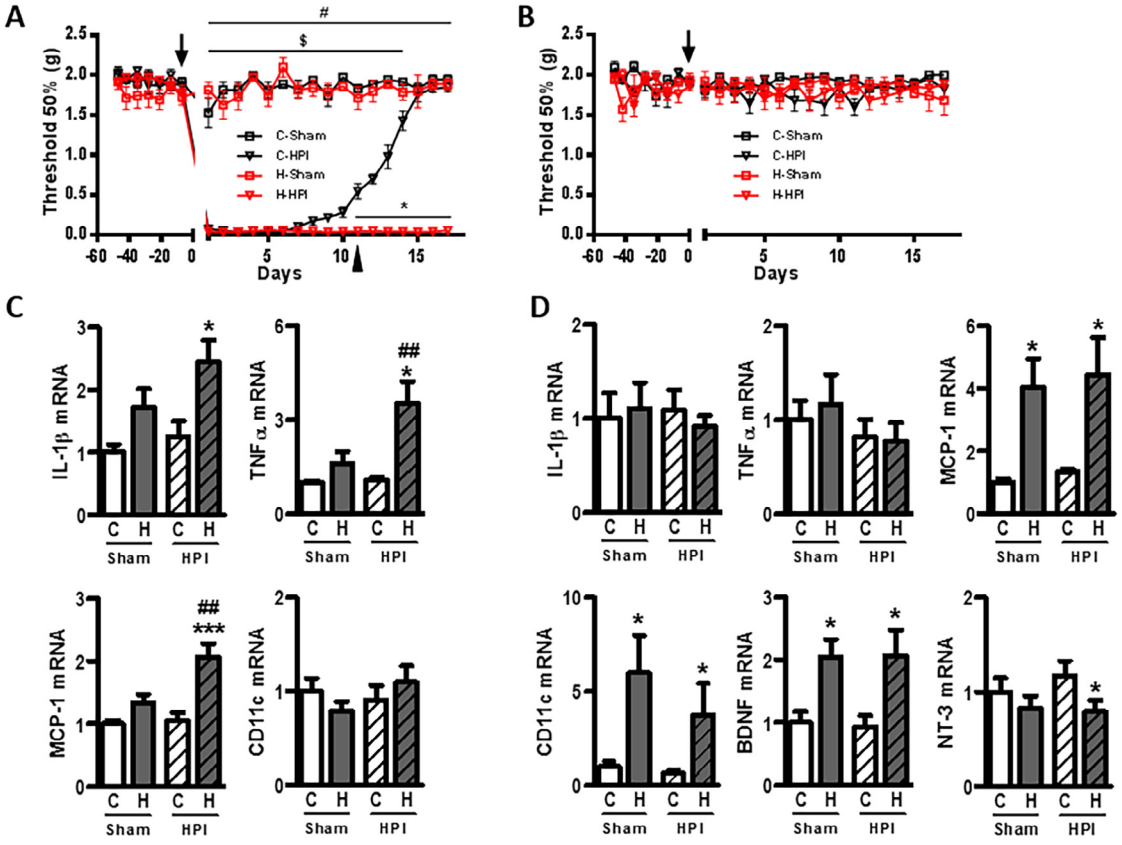


**Fig. 1.** Obesity prolongs pain after hind paw incision. (*A–B*) Withdrawal threshold (measured with von Frey filaments) of the ipsilateral (*A*) and contralateral (*B*) paws of standard chow fed mice (black) and HFD fed mice (red) before and after undergoing a sham operation (□) or a hind paw incision (▽) (marked by an arrow at day 0). The arrow head shows the start of recovery for the chow-fed group that underwent the HPI. All animals were sacrificed 18 days after the sham or HPI surgery. Data are reported as mean ± SEM (n = 10 per group, Two-way ANOVA for repeated measures followed by Tukey's post-hoc test, $P < 0.001, C-Sham vs C-HPI; #P < 0.001, H-Sham vs H-HPI; *P < 0.001, C-HPI vs H-HPI). (*C–D*) Relative mRNA levels of inflammatory markers measured by RT-qPCR in the spinal cord (C) and the ipsilateral sciatic nerve (*D*) of standard chow mice (white columns; C) and HFD mice (grey columns; H) after undergoing a sham operation (unhatched columns; sham) or a hind paw incision (hatched columns; HPI). mRNA levels of the C-Sham group were set at 1. Data are reported as mean ± SEM (n = 10 per group, Two-way ANOVA followed by Tukey's post-hoc test, #P < 0.05, operation effect, **P < 0.01, diet effect). (For interpretation of the references to colour in this figure legend, the reader is referred to the web version of this article.)

an obese phenotype characterized by increased body weight and fat depots (SI Fig. 2A, B). However, while they showed increased hepatic triglyceride and cholesterol contents, HFD-fed mice had similar glycaemia as chow-fed mice (SI Fig. 2C). Furthermore, HFD-fed mice displayed similar expression levels of hepatic enzymes classically altered in diabetes compared to chow-fed animals (SI Fig. 2D). Together these data confirm the obesogenic properties of the HFD used without the onset of a diabetic phenotype.

To study obesity's effects on post-operative pain, HFD-fed (H) and chow-fed (C) mice underwent, 60 days after the beginning of the HFD, either a hind paw incision (HPI) or a sham operation (Sham) (SI Fig. 1). Sham-operated animals (C-Sham and H-Sham) did not experience any change of pain threshold in the ipsilateral paw, measured with von Frey filaments, showing that HFD alone does not impact tactile paw sensitivity (Fig. 1A). HPI-operated groups (C-HPI and H-HPI) presented increased tactile paw sensitivity from day 0. C-HPI mice began recovering from day 11 and were back to their basal paw sensitivity at day 15 consistent with normal pain resolution. In contrast, the H-HPI group did not recover their basal pain threshold up to 17 days post-HPI (Fig. 1A). Finally, in case of mirror-image pain, we measured the pain threshold of the contralateral paw and found it not to be altered by neither operation nor diet (Fig. 1B).

### *3.2. Obesity alters mRNA expression of pro-inflammatory markers and neurotrophins in the spinal cord and sciatic nerve*

We assessed inflammation in the spinal cord (SC), 18 days post-HPI. mRNA expression of neuroexcitatory cytokines (Dinarello, 2011; Grace et al., 2016) such as tumor necrosis factor alpha (TNFα) and interleukin (IL)-1β, and the expression of monocyte chemoattractant protein 1 (MCP-1) were increased in the SC of H-HPI mice (Fig. 1C).

The sciatic nerve (SN) is the relay between the lesion site and the central nervous system (CNS), therefore we also looked at the ipsilateral SN and found levels of MCP-1 and CD11c to be increased by the HFD regardless of the procedure (H-Sham and H-HPI) (Fig. 1D). However, contrary to the SC, IL-1β and TNFα were not increased in the H-HPI group (Fig. 1D).

Neurotrophins are important trophic factors and are able to modulate pain in both central and peripheral nervous systems (Pezet and McMahon, 2006). In the SN, brain-derived neurotrophic factor (BDNF) (a pro-algesic peptide (Li et al., 2008; Ren and Dubner, 2007)) levels were increased by the HFD regardless of the procedure while neurotrophin-3 (NT-3) (an anti-algesic neurotrophin (Gandhi et al., 2004; Wilson-Gerwing et al., 2005)) expression was decreased only for H-HPI mice (Fig. 1D).

In this study, C-HPI mice completely recovered their basal tactile sensitivity, therefore we could only gather limited information on potential differential mechanisms involved in pain resolution in lean and obese mice.

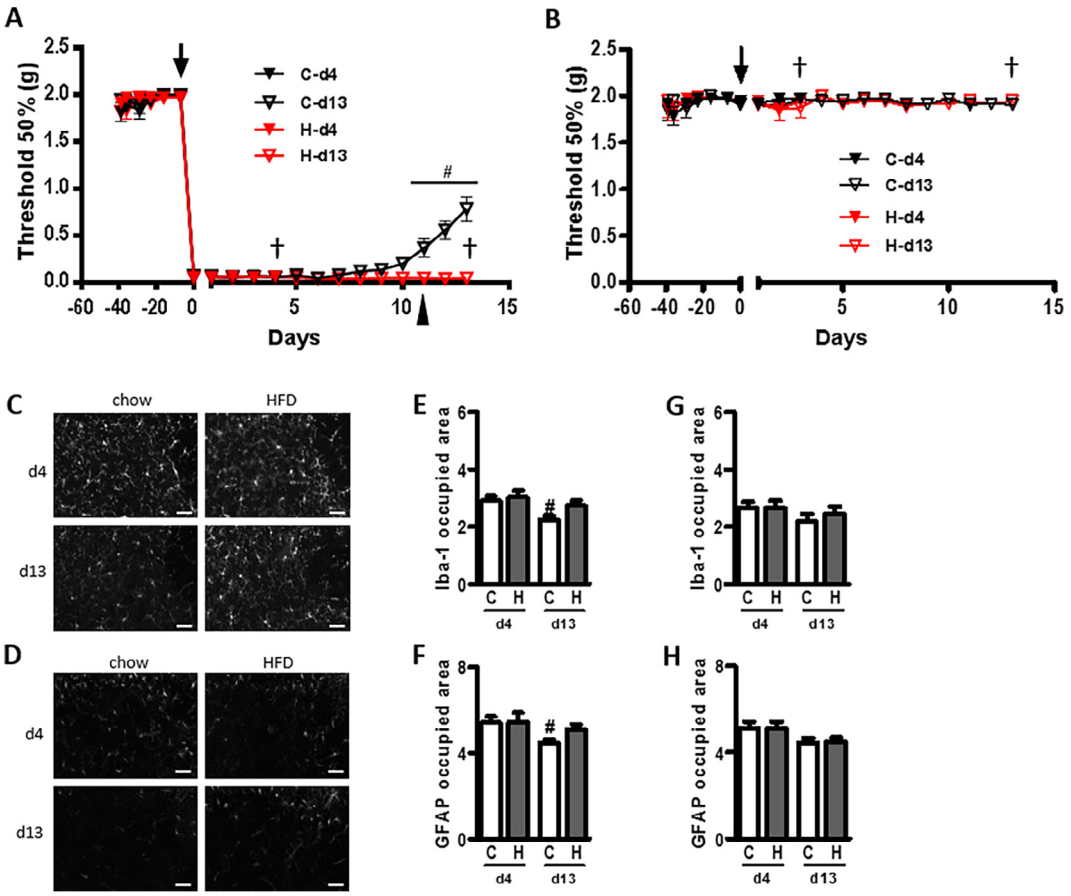


**Fig. 2.** Obesity alters tactile sensitivity and glial activation in the dorsal horn during the recovery phase of postoperative pain. All groups underwent the HPI procedure on day 0. (*A–B*) Standard chow fed mice (black) and HFD fed mice (red) were sacrificed 4 (▼) or 13 (▽) days after the HPI operation. The arrow represents the HPI intervention on day 0. The arrow head shows the start of recovery for the chow-fed group that underwent the HPI. The (†) represents the day of sacrifice of one chow fed and one HFD fed group 4 days after the HPI (d4) and 13 days after the HPI (d13). (*A, B*) Withdrawal threshold of the ipsilateral (*A*) and contralateral (*B*) paws measured with von Frey filaments. Data are reported as mean ± SEM (n = 10 per group, Two-way ANOVA for repeated measures followed by Tukey's post-hoc test for comparison between standard chow fed mice and HFD fed mice at 4 and 13 days post-HPI; and Two-way ANOVA for repeated measures followed by Sidak's post-hoc test for comparison between standard chow fed mice and HFD fed mice at 13 days post-HPI, $^{\#}P < 0.001$, C-d13 vs H-d13). (*C–H*) Representative photomicrographs and quantification of the area occupied by Iba-1 positive cells (microglia) (*C, E*) and GFAP positive cells (astrocytes) (*D, F*) of the ipsilateral dorsal horn of the spinal cord (focused on laminae I and II) (scale bar: 50 μm) of standard chow mice (white columns; C) and HFD mice (grey columns; H) at 4 (d4) or 13 (d13) days post-HPI. (*G–H*) quantification of the area occupied by Iba-1 positive cells (microglia) (*G*) and GFAP positive cells (astrocytes) (*H*) of the contralateral dorsal horn of the spinal cord. Data are reported as mean ± SEM (n = 10 per group, Two-way ANOVA followed by Tukey's post-hoc test, $^{\#}P < 0.05$, time effect). (For interpretation of the references to colour in this figure legend, the reader is referred to the web version of this article.)

### *3.3. Obesity alters glial activation in the spinal cord during post-operative pain*

To study the mechanisms that could explain the obesity-induced prolonged post-operative pain, we performed a new experiment where chow-fed and HFD-fed mice were sacrificed at two different time-points after the HPI procedure (SI Figs. 1 and 3). We chose day 4 post-HPI because both chow-fed and HFD-fed groups display a similar pain threshold and day 13 because chow-fed, but not HFD-fed, mice were in the recovery phase (Fig. 1A). We obtained, in this second study, a similar effect of HFD on tactile paw sensitivity as in the first study for both the ipsi- (Figs. 2A and 1A) and contralateral (Figs. 2B and 1B) paws.

We assessed glial cell (microglia and astrocytes) activation in the L3-5 region of the SC where the SN projects (Rigaud et al., 2008). Indeed, glial cells are directly involved in pain sensitization processes (Ji et al., 2013; Old et al., 2015). We found changes in the areas occupied by Iba-1-positive (microglia) and GFAP-positive (astrocytes) cells in the laminae I and II of the ipsilateral dorsal horn. These were significantly decreased in chow-fed mice at day 13 (C-d13) compared with day 4 (C-d4) but remained unchanged in HFD mice between day 4 (H-d4) and day 13 (H-d13) (Fig. 2C–F). Besides, we also found a trend towards an increase of the area occupied for both Iba-1 and GFAP positive cells at day 13 for HFD (H-d13) mice compared to chow-fed mice (C-d13) but only for the ipsilateral side. Therefore, the decrease in microglia and astrocyte activation was restricted to the ipsilateral side of the SC (Fig. 2G–H) and to lean animals at day 13 post-HPI.

When looking at inflammatory markers' expression in the SC, IL-1β expression was increased by obesity at day 13 (Fig. 3A). However, obesity had no impact on neurotrophins expression in this tissue (Fig. 3B). The brainstem is another central structure involved in pain control. However, we found no HFD-induced variations in inflammatory marker and neurotrophin expression in the brainstem (SI Fig. 4A–B).

### *3.4. Obesity exacerbates the inflammatory response and alters neurotrophin expression in the sciatic nerve during post-operative pain*

We also studied obesity's effects on the SN. TNFα and the macrophage marker F4/80 were increased by the HFD 4 days after the HPI compared with chow-fed mice and their levels were lower in H-d13 mice compared with H-d4 (Fig. 3C). MCP-1 and BDNF levels were

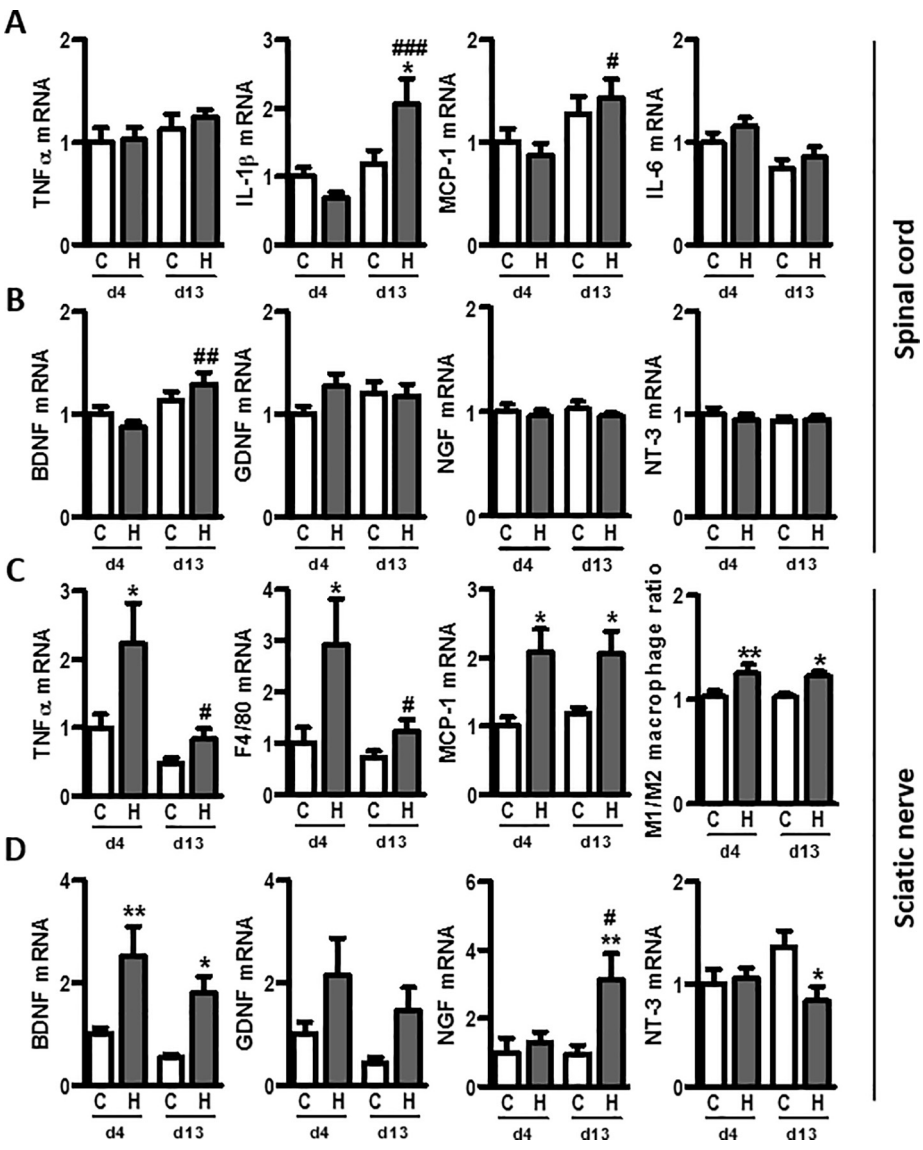


**Fig. 3.** Obesity alters spinal and sciatic inflammation during the recovery phase of post-operative pain. All groups underwent the HPI procedure on day 0. Relative mRNA levels in the spinal cord of inflammatory markers (*A*) and neurotrophins (*B*), and relative mRNA levels in the ipsilateral sciatic nerve of inflammatory markers (*C*) and neurotrophins (*D*) measured by RT-qPCR of standard chow fed mice (white columns; C) and HFD fed mice (grey columns; H) and sacrificed 4 (d4) or 13 (d13) days post-HPI. mRNA levels of the C-d4 group were set at 1. Data are mean ± SEM (n = 10 per group, Two-way ANOVA followed by Tukey's post-hoc test, $^{*}P < 0.05$, $^{**}P < 0.01$, diet effect; $^{\#}P < 0.05$, $^{\#\#}P < 0.01$, $^{\#\#\#}P < 0.001$, time effect).

increased by the HFD at both time-points. Interestingly, expression of nerve growth factor (NGF), another pro-algesic neurotrophin (Mizumura and Murase, 2015), was increased, while the anti-algesic NT-3 was decreased, in H-d13 mice (Fig. 3C–D). Finally, because both MCP-1 and F4/80 were increased, indicating the recruitment and increased presence of macrophages, we measured the activation state of SN-associated macrophages and found a more pronounced polarization towards a M1-like pro-inflammatory state (assessed with CD11c) than M2-like activation (assessed with arginase 1) in HFD-fed mice at both time-points compared with their respective control (Fig. 3C).

As variations of inflammatory markers and neurotrophins were similar in the SN (Fig. 3C–D), we looked for potential correlations. Expression of MCP-1 and BDNF, TNFα and BDNF, as well as TNFα and glial cell line-derived neurotrophic factor (GDNF) were correlated in both the first and second studies (SI Table 1).

To support these correlations and to investigate a potential link between SN inflammation and neurotrophin expression, we incubated SN explants with or without lipopolysaccharides (LPS). We used a low dose of LPS (10 ng/ml) in pursuance of mimicking the obesity-induced low-grade endotoxemia (Cani et al., 2012). Beside the expected increase of pro-inflammatory markers (IL-6, TNFα and MCP-1) (Fig. 4A), expression of the pro-algesic neurotrophins NGF and BDNF was increased while GDNF was unchanged in LPS-activated SN explants compared with control (Fig. 4B).

### 3.5. Obesity does not alter paw inflammation during post-operative pain

Differential healing at the surgery site could directly participate in the prolonged pain measured in HFD mice. We found no macroscopic changes in the wound itself, nor differences in wound-healing duration between chow-fed and HFD-fed mice at days 4 or 13 (data not shown). This was further confirmed by the measure in paw skin of vascular endothelial growth factor A (VEGFa) and stromal cell-derived factor 1 (SDF-1) mRNA expression, two markers classically associated with impaired wound healing (Botusan et al., 2008; Canesso et al., 2014). While VEGFa expression was not influenced by the diet, it was altered between day 4 and 13, and the same trend was observed for SDF-1, consistent with the different phases of wound healing (SI Fig. 4D) (Bitto et al., 2008; Gu et al., 2013; Lima et al., 2012). Transient inflammation is also present in the paw of lesioned animals. Here, the inflammatory markers (IL-6, MCP-1 and F4/80) were decreased at day 13 compared to day 4 (SI Fig. 4E) although this did not reach statistical significance

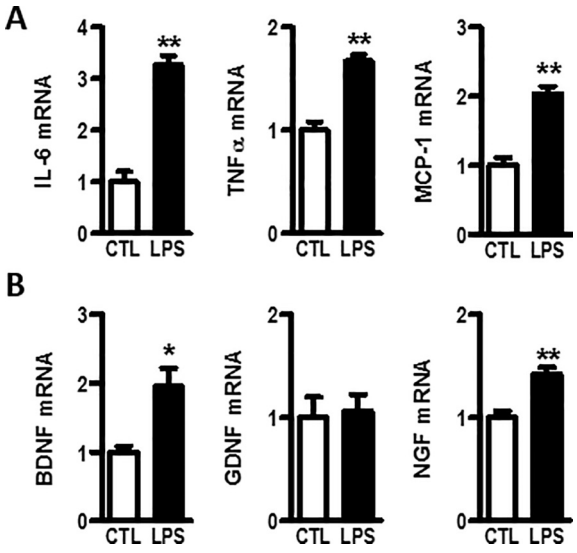


**Fig. 4.** Sciatic nerve explants express higher levels of BDNF and NGF mRNA upon LPS activation. Relative mRNA levels of inflammatory markers (*A*) and neurotrophins (*B*) measured by RT-qPCR in sciatic nerve explants treated either with vehicle or LPS (10 ng/ml) for 6 h. mRNA levels of the vehicle-treated group were set at 1 (n = 5 per group, two-tailed Mann-Whitney test, $^{**}$, $P < 0.01$).

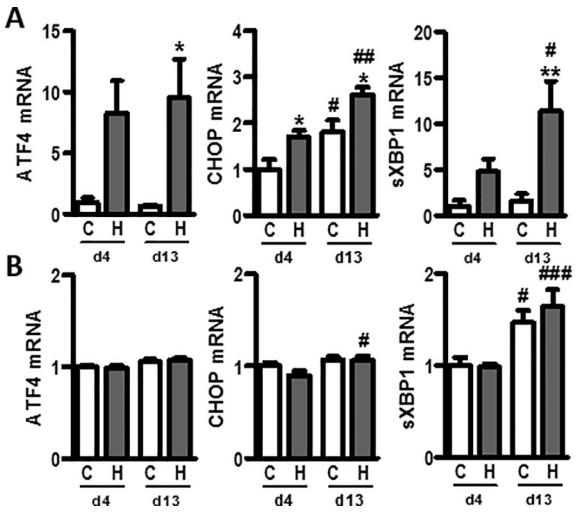


**Fig. 5.** Endoplasmic reticulum stress is increased by both obesity and time in the sciatic nerve and the spinal cord. All groups underwent the HPI procedure on day 0. Relative mRNA levels of ER stress proteins measured by RT-qPCR in the ipsilateral sciatic nerve (*A*) and spinal cord (*B*) of standard chow mice (white columns; C) and HFD mice (grey columns; H) sacrificed 4 (d4) or 13 (d13) days post HPI. mRNA levels of the C-d4 group were set at 1. Data are mean ± SEM (n = 10 per group, Two-way ANOVA followed by Tukey's post hoc test, $^{*}P < 0.05$, $^{**}P < 0.01$, diet effect; $^{\#}P < 0.05$, $^{\#\#}P < 0.01$, $^{\#\#\#}P < 0.001$, time effect).

for IL-6 (CTL group) or MCP-1 (HFD group) and no effect of the diet was observed except for MCP-1 at 4 days post-HPI. Finally, NT-3 expression was increased for C-d13 mice compared with C-d4 mice (SI Fig. 4F).

### 3.6. Endoplasmic reticulum (ER) stress is increased by obesity during post-operative pain

Recently, ER stress was shown to be directly involved in the altered pain perception of type I diabetic mice (Inceoglu et al., 2015). Thus, we wondered if obesity would induce alterations in the expression of ER stress markers in HPI mice. We used mRNA expression of activating transcription factor 4 (ATF4), C/EBP homologous protein (CHOP) and spliced X box-binding protein 1 (sXBP1), which are widely used as ER stress markers and were shown to correlate with the protein levels (Inceoglu et al., 2015). In the SN, ATF4 and sXBP1 expression were increased in H-d13 compared with C-d13 mice. sXBP1 expression was also significantly increased in H-d13 compared with H-d4 mice. CHOP expression in the SN was increased with both time and HFD (Fig. 5A). Variations were less marked in the SC, but we found a significant increase of CHOP in H-d13 mice compared with H-d4 while sXBP1 expression was increased over time regardless of the diet (Fig. 5B). Finally, in the paw skin and brainstem, we found no variation induced by diet-induced obesity besides an increase of ATF4 expression in the paw skin at day 13 (SI Fig. 4C and G).

### 3.7. Diet modulation rescues aberrant pain perception induced by obesity

Our data clearly show that obesity affects recovery duration in post-operative pain. We wondered what would happen to obese animals experiencing post-operative pain for a longer period and if a diet switch mimicking a perioperative dietary restriction in humans, could restore normal tactile paw sensitivity. Therefore, we performed the HPI procedure on three groups of mice fed a HFD for 60 days (third study, see SI Fig. 1). One group was switched to standard chow on the day of the surgery (H-C d0), another group was switched to standard chow 10 weeks post-HPI (H-C) and the remaining group was kept under HFD during the entire experiment (H-H) (SI Figs. 1 and 5A). When comparing these latter two groups, we found a clear normalization in fat depots size and hepatic triglyceride and cholesterol levels for H-C mice (SI Fig. 5B–C). H-C d0 mice started to recover from day 24 (compared to day 11 for chow-fed mice (Fig. 1A)) and reached their basal pain threshold 35 days post-surgery (Fig. 6A). H-C mice started to recover from day 124 (53 days post diet switch) and reached their basal pain threshold on day 131 post-HPI (Fig. 6A). Finally, mice fed a HFD throughout the study (H-H) experienced pain for 162 days post-HPI and displayed no signs of improvement at the end of this study (Fig. 6A). Interestingly, the time between diet switch and postoperative pain normalization is function of the total duration of HFD exposure. Indeed, H-C d0 mice needed around 35 days to recover their basal tactile sensitivity whereas H-C mice needed 58 days post-diet switch to recover their basal tactile sensitivity (Fig. 6A & SI Fig. 5A). The withdrawal pain threshold for the contralateral paw did not differ between the three groups of mice supporting the lack of effect of a HFD on paw sensitivity on its own (Fig. 6B). We also assessed glial cell activation in the dorsal horn of the SC in the ipsi- and contra-lateral laminae I and II and found a trend towards a decrease of the area occupied by microglia for H-C mice compared with H-H mice (Fig. 6C–D). Finally, we measured the expression of inflammatory markers, neurotrophins, and ER stress markers in the SN of H-H and H-C mice. We found a significant decrease in the expression of MCP-1, F4/80, BDNF and NT-3 with the diet switch (Fig. 7A–C). Regarding the SC, no significant changes were measured for inflammatory markers or neurotrophins (Fig. 7D–F).

## 4. Discussion

When facing post-operative pain in the HPI model, mice fed a standard chow recovered quickly their basal paw sensitivity which is consistent with the literature (Brennan et al., 1996). However, we showed that mice fed a HFD before and after the operation experienced pain for a much longer time compared with chow-fed mice (at least 162 days vs 14 days, respectively). This finding is of importance considering the worldwide incidence of obesity. Interestingly, a diet intervention (from HFD to standard chow) could rescue hyperalgesia and restore basal paw sensitivity.

The prolonged pain experienced by obese mice does not seem to be an effect of some component of the HFD. If it were the case, we would expect an improvement of pain sensitivity shortly after the diet switch

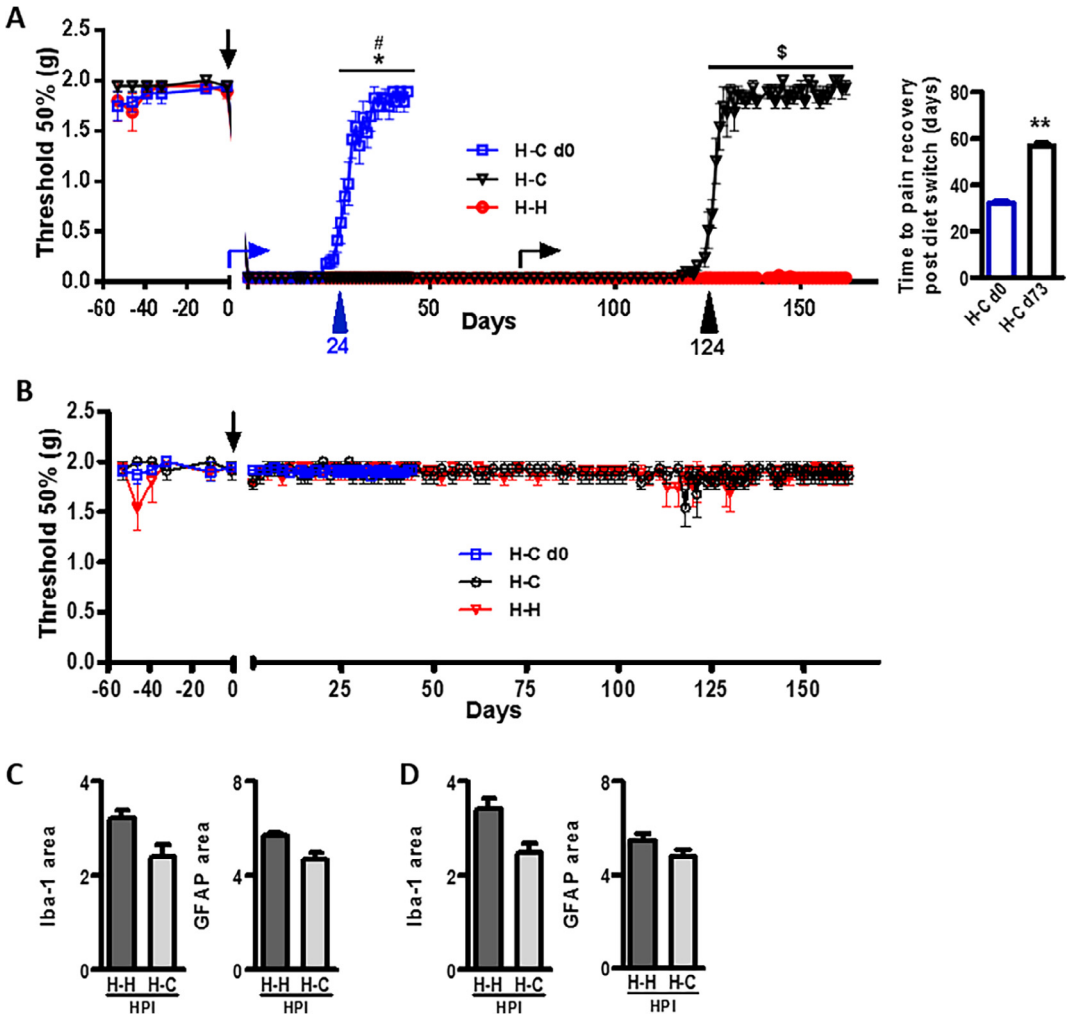


**Fig. 6.** Diet switch to standard chow rescues obese mice post-operative pain. (*A–B*) Withdrawal threshold (measured with von Frey filaments) of the ipsilateral (A) and contralateral (B) paws of HFD fed mice switched to standard chow on day 0 of the HPI operation (blue; H–C d0), HFD fed mice switched to standard chow 10 weeks post-HPI (black; H-C) and mice fed a HFD throughout the entire experiment (red; H-H). The vertical arrow represents the HPI intervention on day 0 and the horizontal arrows the diet interventions at day 0 (blue) and 10 weeks post-HPI (black). The blue arrow head shows the start of recovery for the H-C d0 group. The black arrow head shows the start of recovery for the H-C group. Data are reported as mean ± SEM (n = 10 for HFD mice switched to standard chow on day 0 and n = 5 for the two remaining groups, Two-way ANOVA for repeated measures followed by Tukey's post-hoc test for comparison between the 3 groups, $^{*}P < 0.001$, H-C d0 vs H-H; $^{\#}P < 0.001$, H-C d0 vs H-C; and Two-way ANOVA for repeated measures followed by Sidak's post-hoc test for comparison between H-C vs H-H, $\$P < 0.001$). (*C–D*) Quantification of the area occupied by Iba-1 positive cells (microglia) and GFAP positive cells (astrocytes) of the ipsilateral (*C*) and contralateral (*D*) dorsal horn of the spinal cord (focused on laminae I and II) of mice fed a HFD throughout the entire experiment (dark grey; H-H) and HFD mice switched to standard chow 10 weeks post-HPI (light grey; H-C) and sacrificed 162 days after the HPI surgery. (For interpretation of the references to colour in this figure legend, the reader is referred to the web version of this article.)

as well as a similar time to recover from post-operative pain following the switches of day 0 post-HPI and 10 weeks post-HPI. In fact, the prolonged pain seems more likely linked to obesity-induced metabolic alterations. Indeed, the longer mice are fed a HFD, the longer it takes to recover their basal pain threshold. This hypothesis is also supported by the fact that mice recovered their basal pain threshold several weeks after having lost weight (Fig. 6A and SI Fig. 5A).

Focusing on day 4 and 13 post-HPI enabled us to investigate the temporality of the processes at play in the persistent post-operative pain in obese mice and allowed us to identify the SN and SC as key tissues involved in the prolonged post-operative pain, indicating that obesity disrupts the homeostasis of both peripheral and central nervous systems. Conversely, the injured skin does not play a major role in the extended obesity-induced post-operative pain as inflammatory markers' variations in the paw skin were mainly dependent on temporality and not on diet. However, the SN and the SC display some variations in inflammatory markers' expression that are only dependent on diet and specifically at the later time-point, hence underlying potential mechanisms involved in prolonged post-operative pain in obesity. Besides inflammatory markers, neurotrophins are involved in a plethora of mechanisms of the nervous system ranging from survival and cell death to pain processes (Park and Poo, 2013; Pezet and McMahon, 2006). Interestingly, neurotrophin expression was influenced by both diet and temporality. In the SN, the pro-algesic peptide BDNF (Ding et al., 2015; Li et al., 2008; Ren and Dubner, 2007) was increased by the HFD at both time-points and could explain the prolonged pain experienced by these mice, especially as its expression was decreased by the diet-switch. NGF (another pro-algesic neurotrophin (Mizumura *et al.*, 2015)) and NT-3 (an anti-algesic neurotrophin (Gandhi et al., 2004; Watanabe et al., 2000; Wilson-Gerwing et al., 2005)) could also explain the delayed recovery of HFD-fed mice. Indeed, NGF was increased at day 13 in HFD-fed mice whereas NT-3 was decreased (Fig. 3D). Thus, changes in both neurotrophins and inflammation in the SN seem to be key features in the prolonged post-operative pain endured by obese mice.

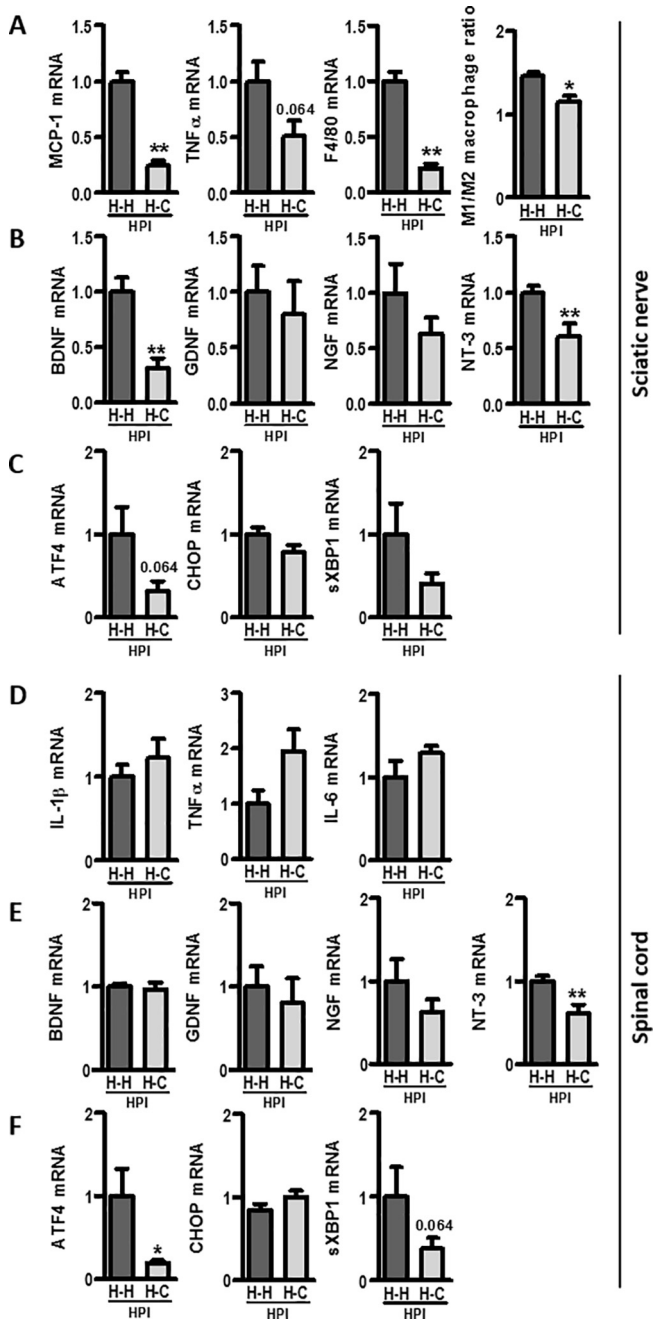


**Fig. 7.** Diet switch to standard chow rescues some inflammatory parameters in the sciatic nerve and spinal cord. (*A–B*) Relative mRNA levels of inflammatory markers (A) and neurotrophins (*B*) measured by RT-qPCR in the ipsilateral sciatic nerve of mice fed a HFD throughout the entire experiment (dark grey; H-H) and HFD mice switched to standard chow 10 weeks post-HPI (light grey; H-C). Mice of both groups were sacrificed 162 days after the HPI surgery. mRNA levels of the H-H group were set at 1 (n = 5 per group, two-tailed Mann-Whitney test, $^{**}P < 0.01$). (*C–E*) Relative mRNA levels of inflammatory markers (*C*), neurotrophins (*D*) and ER stress proteins (*E*) measured by RT-qPCR in the spinal cord of mice fed a HFD throughout the entire experiment (dark grey columns; H-H) and HFD fed mice switched to standard chow 10 weeks post-HPI (light grey columns; H-C). Mice of both groups were sacrificed 162 days after the HPI surgery. mRNA levels of the H-H group were set at 1 (n = 5 per group, two-tailed Mann-Whitney test, $^{*}P < 0.05$ and $^{**}P < 0.01$).

These elements appear to be interrelated as we found positive correlations between inflammatory markers and neurotrophins and that incubation of SN explants with LPS increased the expression of BDNF and NGF. This potential link between inflammation and endogenous mediators of pain is of importance in the context of obesity-associated pain. Indeed, we and others have shown that obesity and metabolic syndrome are characterized by a low-grade inflammation affecting both the periphery and the CNS (Cani et al., 2007; Guillemot-Legris et al., 2016b; Monteiro and Azevedo, 2010), which is partly the consequence of increased circulating LPS (Cani et al., 2007; Cani et al., 2008).

Besides inflammation and neurotrophin expression, ER stress is increased in the SN. This physiological process was recently implicated in the regulation of pain perception in a model of diabetic neuropathic pain, as well as in models of neuropathic and inflammatory pain (Inceoglu et al., 2015; Yang et al., 2014; Zhang et al., 2015). Here, HFD-feeding was sufficient to induce ER stress in the SN in a post-operative setting. Moreover, diet-intervention decreased ER stress markers further suggesting its involvement in the prolonged pain experienced by obese animals.

Central sensitization is a mechanism of pain modulation in chronic and prolonged settings where astrocytes and microglia activation represent a key feature (Dirks et al., 2002; Ji et al., 2013; Latremoliere and Woolf, 2009). Here, while the activation of astrocytes and microglia was decreased in chow-fed mice on day 13 post-HPI, these inflammatory cells of the CNS were still activated at day 13 for HFD mice. The prolonged activation state of the glial cells in HFD-fed mice could also explain the chronicization of post-operative pain.

Finally, as some studies show that pain mechanisms (e.g. receptors or immune cells involved) differ between male and female (Brings and Zylka, 2015; Wiesenfeld-Hallin, 2005) it could be interesting to study the impact of obesity in post-operative pain in female mice as well.

In conclusion, we show that obesity-induced prolonged post-operative pain is a multifactorial process involving (i) sustained glial cell activation in the SC, (ii) increased expression of inflammatory markers and macrophage activation in the SN, (iii) increased expression of pro-algesic neurotrophins as well as (iv) increased ER stress in the SN and SC of obese mice. All of these identified mechanisms warrant further studies in order to determine their separate relevance as well as their individual impact in this specific context. Here, we demonstrate that a « simple » diet intervention leading to a weight loss results in a decrease of inflammation and macrophage activation as well as in a decrease in neurotrophin expression and ER stress markers. This was accompanied by the resolution of the prolonged diet-induced post-operative pain. This is of high interest from a translational point and clearly deserves to be assessed in the clinical context.

## Acknowledgments

OGL was supported by a fellowship from the “Fonds pour la recherche dans l'industrie et l'agriculture” (FRIA, Belgium) and a recipient of the “Bourse du Patrimoine” (Université catholique de Louvain, Belgium). MA and OGL are postdoctoral researchers from the FRS-FNRS (Fonds de la Recherche Scientifique), Belgium. GGM is the recipient of research grants from the Fonds Spéciaux de Recherches (FSR, Université catholique de Louvain) and from the FRS-FNRS, Belgium.

## Author contributions

OGL: designed and performed experiments, analyzed the data, interpreted the results and wrote the manuscript ; BB: performed experiments, analyzed the data and contributed to writing the manuscript; VM : performed experiments ; RD : performed experiments and contributed to writing the manuscript; EH: provided reagents and contributed to writing the manuscript; MA: participated to the design of the experiments, performed experiments, interpreted the results and contributed to writing the manuscript; GGM: conceived and supervised the project, designed the experiments, interpreted the results and wrote the manuscript.

## Competing interests

The authors declare no competing interest.

## Appendix A. Supplementary data

Supplementary data associated with this article can be found, in the online version, at https://doi.org/10.1016/j.bbi.2018.07.022.

## References


Alhouayek, M., Masquelier, J., Cani, P.D., Lambert, D.M., Muccioli, G.G., 2013. Implication of the anti-inflammatory bioactive lipid prostaglandin D2-glycerol ester in the control of macrophage activation and inflammation by ABHD6. Proc. Natl. Acad. Sci. U.S.A 110, 17558–17563.

Bitto, A., Minutoli, L., Altavilla, D., Polito, F., Fiumara, T., Marini, H., Galeano, M., Calo, M., Lo, C.P., Bonaiuto, M., Migliorato, A., Caputi, A.P., Squadrito, F., 2008. Simvastatin enhances VEGF production and ameliorates impaired wound healing in experimental diabetes. Pharmacol. Res. 57, 159–169.

Botusan, I.R., Sunkari, V.G., Savu, O., Catrina, A.I., Grunler, J., Lindberg, S., Pereira, T., Yla-Herttuala, S., Poellinger, L., Brismar, K., Catrina, S.B., 2008. Stabilization of HIF-1alpha is critical to improve wound healing in diabetic mice. Proc. Natl. Acad. Sci. U.S.A 105, 19426–19431.

Brennan, T.J., Vandermeulen, E.P., Gebhart, G.F., 1996. Characterization of a rat model of incisional pain. Pain 64, 493–501.

Brings, V.E., Zylka, M.J., 2015. Sex, drugs and pain control. Nat. Neurosci. 18, 1059–1060.

Canesso, M.C., Vieira, A.T., Castro, T.B., Schirmer, B.G., Cisalpino, D., Martins, F.S., Rachid, M.A., Nicoli, J.R., Teixeira, M.M., Barcelos, L.S., 2014. Skin wound healing is accelerated and scarless in the absence of commensal microbiota. J. Immunol. 193, 5171–5180.

Cani, P.D., Amar, J., Iglesias, M.A., Poggi, M., Knauf, C., Bastelica, D., Neyrinck, A.M., Fava, F., Tuohy, K.M., Chabo, C., Waget, A., Delmee, E., Cousin, B., Sulpice, T., Chamontin, B., Ferrieres, J., Tanti, J.F., Gibson, G.R., Casteilla, L., Delzenne, N.M., Alessi, M.C., Burcelin, R., 2007. Metabolic endotoxemia initiates obesity and insulin resistance. Diabetes 56, 1761–1772.

Cani, P.D., Bibiloni, R., Knauf, C., Waget, A., Neyrinck, A.M., Delzenne, N.M., Burcelin, R., 2008. Changes in gut microbiota control metabolic endotoxemia-induced inflammation in high-fat diet-induced obesity and diabetes in mice. Diabetes 57, 1470–1481.

Cani, P.D., Osto, M., Geurts, L., Everard, A., 2012. Involvement of gut microbiota in the development of low-grade inflammation and type 2 diabetes associated with obesity. Gut Microbes. 3, 279–288.

Chaplan, S.R., Bach, F.W., Pogrel, J.W., Chung, J.M., Yaksh, T.L., 1994. Quantitative assessment of tactile allodynia in the rat paw. J. Neurosci. Methods 53, 55–63.

Chapman, C.R., Vierck, C.J., 2017. The transition of acute postoperative pain to chronic pain: an integrative overview of research on mechanisms. J. Pain 18, 359.

DeFronzo, R.A., Ferrannini, E., Groop, L., Henry, R.R., Herman, W.H., Holst, J.J., Hu, F.B., Kahn, C.R., Raz, I., Shulman, G.I., Simonson, D.C., Testa, M.A., Weiss, R., 2015. Type 2 diabetes mellitus. Nat. Rev. Dis. Primers 1, 15019.

Deumens, R., Steyaert, A., Forget, P., Schubert, M., Lavand'homme, P., Hermans, E., De, K.M., 2013. Prevention of chronic postoperative pain: cellular, molecular, and clinical insights for mechanism-based treatment approaches. Prog. Neurobiol. 104, 1–37.

Dinarello, C.A., 2011. A clinical perspective of IL-1beta as the gatekeeper of inflammation. Eur. J. Immunol. 41, 1203–1217.

Ding, X., Cai, J., Li, S., Liu, X.D., Wan, Y., Xing, G.G., 2015. BDNF contributes to the development of neuropathic pain by induction of spinal long-term potentiation via SHP2 associated GluN2B-containing NMDA receptors activation in rats with spinal nerve ligation. Neurobiol. Dis. 73, 428–451.

Dirks, J., Moiniche, S., Hilsted, K.L., Dahl, J.B., 2002. Mechanisms of postoperative pain: clinical indications for a contribution of central neuronal sensitization. Anesthesiology 97, 1591–1596.

Esser, N., Legrand-Poels, S., Piette, J., Scheen, A.J., Paquot, N., 2014. Inflammation as a link between obesity, metabolic syndrome and type 2 diabetes. Diabetes Res. Clin. Pract. 105, 141–150.

Everard, A., Geurts, L., Caesar, R., Van, H.M., Matamoros, S., Duparc, T., Denis, R.G., Cochez, P., Pierard, F., Castel, J., Bindels, L.B., Plovier, H., Robine, S., Muccioli, G.G., Renauld, J.C., Dumoutier, L., Delzenne, N.M., Luquet, S., Backhed, F., Cani, P.D., 2014. Intestinal epithelial MyD88 is a sensor switching host metabolism towards obesity according to nutritional status. Nat. Commun. 5, 5648.

Gandhi, R., Ryals, J.M., Wright, D.E., 2004. Neurotrophin-3 reverses chronic mechanical hyperalgesia induced by intramuscular acid injection. J. Neurosci. 24, 9405–9413.

Grace, P.M., Strand, K.A., Galer, E.L., Urban, D.J., Wang, X., Baratta, M.V., Fabisiak, T.J., Anderson, N.D., Cheng, K., Greene, L.I., Berkelhammer, D., Zhang, Y., Ellis, A.L., Yin, H.H., Campeau, S., Rice, K.C., Roth, B.L., Maier, S.F., Watkins, L.R., 2016. Morphine paradoxically prolongs neuropathic pain in rats by amplifying spinal NLRP3 inflammasome activation. Proc. Natl. Acad. Sci. U.S.A 113, E3441–E3450.

Gu, X.Y., Shen, S.E., Huang, C.F., Liu, Y.N., Chen, Y.C., Luo, L., Zeng, Y., Wang, A.P., 2013. Effect of activated autologous monocytes/macrophages on wound healing in a rodent model of experimental diabetes. Diabetes Res. Clin. Pract. 102, 53–59.

Guillemot-Legris, O., Masquelier, J., Everard, A., Cani, P.D., Alhouayek, M., Muccioli, G.G., 2016a. High-fat diet feeding differentially affects the development of inflammation in the central nervous system. J. Neuroinflammation 13, 206.

Guillemot-Legris, O., Mutemberezi, V., Cani, P.D., Muccioli, G.G., 2016b. Obesity is associated with changes in oxysterol metabolism and levels in mice liver, hypothalamus, adipose tissue and plasma. Sci. Rep. 6, 19694.

Hoeber, J., Trolle, C., Konig, N., Du, Z., Gallo, A., Hermans, E., Aldskogius, H., Shortland, P., Zhang, S.C., Deumens, R., Kozlova, E.N., 2015. Human embryonic stem cell-derived progenitors assist functional sensory axon regeneration after dorsal root avulsion injury. Sci. Rep. 5, 10666.

Inceoglu, B., Bettaieb, A., Trindade da Silva, C.A., Lee, K.S., Haj, F.G., Hammock, B.D., 2015. Endoplasmic reticulum stress in the peripheral nervous system is a significant driver of neuropathic pain. Proc. Natl. Acad. Sci. U.S.A 112, 9082–9087.

Jang, J.H., Liang, D., Kido, K., Sun, Y., Clark, D.J., Brennan, T.J., 2011. Increased local concentration of complement C5a contributes to incisional pain in mice. J. Neuroinflammation 8, 80.

Ji, R.R., Berta, T., Nedergaard, M., 2013. Glia and pain: is chronic pain a gliopathy? Pain 154 (Suppl. 1), S10–S28.

Kehlet, H., Jensen, T.S., Woolf, C.J., 2006. Persistent postsurgical pain: risk factors and prevention. Lancet 367, 1618–1625.

Latremoliere, A., Woolf, C.J., 2009. Central sensitization: a generator of pain hypersensitivity by central neural plasticity. J. Pain 10, 895–926.

Li, C.Q., Xu, J.M., Liu, D., Zhang, J.Y., Dai, R.P., 2008. Brain derived neurotrophic factor (BDNF) contributes to the pain hypersensitivity following surgical incision in the rats. Mol. Pain 4, 27.

Lima, M.H., Caricilli, A.M., de Abreu, L.L., Araujo, E.P., Pelegrinelli, F.F., Thirone, A.C., Tsukumo, D.M., Pessoa, A.F., dos Santos, M.F., de Moraes, M.A., Carvalheira, J.B., Velloso, L.A., Saad, M.J., 2012. Topical insulin accelerates wound healing in diabetes by enhancing the AKT and ERK pathways: a double-blind placebo-controlled clinical trial. PLoS One 7, e36974.

Lu, W., Hagiwara, D., Morishita, Y., Tochiya, M., Azuma, Y., Suga, H., Goto, M., Banno, R., Sugimura, Y., Oyadomari, S., Mori, K., Arima, H., 2016. Unfolded protein response in hypothalamic cultures of wild-type and ATF6alpha-knockout mice. Neurosci. Lett. 612, 199–203.

Lumeng, C.N., Saltiel, A.R., 2011. Inflammatory links between obesity and metabolic disease. J. Clin. Invest. 121, 2111–2117.

Mizumura, K., Murase, S., 2015. Role of nerve growth factor in pain. Handb. Exp. Pharmacol. 227, 57–77.

Monteiro, R., Azevedo, I., 2010. Chronic inflammation in obesity and the metabolic syndrome. Mediators Inflammation 2010.

O'Neill, S., O'Driscoll, L., 2015. Metabolic syndrome: a closer look at the growing epidemic and its associated pathologies. Obes. Rev. 16, 1–12.

Old, E.A., Clark, A.K., Malcangio, M., 2015. The role of glia in the spinal cord in neuropathic and inflammatory pain. Handb. Exp. Pharmacol. 227, 145–170.

Park, H., Poo, M.M., 2013. Neurotrophin regulation of neural circuit development and function. Nat. Rev. Neurosci. 14, 7–23.

Peltier, A., Goutman, S.A., Callaghan, B.C., 2014. Painful diabetic neuropathy. BMJ 348, g1799.

Pezet, S., McMahon, S.B., 2006. Neurotrophins: mediators and modulators of pain. Annu. Rev. Neurosci. 29, 507–538.

Rajamaki, T.J., Jamsen, E., Puolakka, P.A., Nevalainen, P.I., Moilanen, T., 2015. Diabetes is associated with persistent pain after hip and knee replacement. Acta Orthop. 86, 586–593.

Reddi, D., Curran, N., 2014. Chronic pain after surgery: pathophysiology, risk factors and prevention. Postgrad. Med. J. 90, 222–227.

Ren, K., Dubner, R., 2007. Pain facilitation and activity-dependent plasticity in pain modulatory circuitry: role of BDNF-TrkB signaling and NMDA receptors. Mol. Neurobiol. 35, 224–235.

Rigaud, M., Gemes, G., Barabas, M.E., Chernoff, D.I., Abram, S.E., Stucky, C.L., Hogan, Q.H., 2008. Species and strain differences in rodent sciatic nerve anatomy: implications for studies of neuropathic pain. Pain 136, 188–201.

Sandkuhler, J., 2009. Models and mechanisms of hyperalgesia and allodynia. Physiol. Rev. 89, 707–758.

Wang, Y.C., McPherson, K., Marsh, T., Gortmaker, S.L., Brown, M., 2011. Health and economic burden of the projected obesity trends in the USA and the UK. Lancet 378, 815–825.

Watanabe, M., Endo, Y., Kimoto, K., Katoh-Semba, R., Arakawa, Y., 2000. Inhibition of adjuvant-induced inflammatory hyperalgesia in rats by local injection of neurotrophin-3. Neurosci. Lett. 282, 61–64.

White, F.A., Bhangoo, S.K., Miller, R.J., 2005. Chemokines: integrators of pain and inflammation. Nat. Rev. Drug Discovery 4, 834–844.

Wiesenfeld-Hallin, Z., 2005. Sex differences in pain perception. Gend. Med. 2, 137–145.

Wilson-Gerwing, T.D., Dmyterko, M.V., Zochodne, D.W., Johnston, J.M., Verge, V.M., 2005. Neurotrophin-3 suppresses thermal hyperalgesia associated with neuropathic pain and attenuates transient receptor potential vanilloid receptor-1 expression in adult sensory neurons. J. Neurosci. 25, 758–767.

Yang, E.S., Bae, J.Y., Kim, T.H., Kim, Y.S., Suk, K., Bae, Y.C., 2014. Involvement of endoplasmic reticulum stress response in orofacial inflammatory pain. Exp. Neurobiol. 23, 372–380.

Zhang, E., Yi, M.H., Shin, N., Baek, H., Kim, S., Kim, E., Kwon, K., Lee, S., Kim, H.W., Chul, B.Y., Kim, Y., Kwon, O.Y., Lee, W.H., Kim, D.W., 2015. Endoplasmic reticulum stress impairment in the spinal dorsal horn of a neuropathic pain model. Sci. Rep. 5, 11555.